JOURNAL OF GEOPHYSICAL RESEARCH, VOL. 107, NO. D24, 4800, doi:10.1029/2002JD002483, 2002

Sensitivity of tracer transports and stratospheric ozone to sea surface temperature patterns in the doubled CO_2 climate

David Rind, Jean Lerner, and Judith Perlwitz
Goddard Institute for Space Studies at Columbia University, New York, New York, USA

Chris McLinden
Air Quality Research Branch, Meteorological Service of Canada, Downsview, Ontario, Canada

Michael Prather
Earth Systems Science Department, University of California, Irvine, Irvine, California, USA

Received 26 April 2002; revised 30 July 2002; accepted 1 August 2002; published 28 December 2002.

[1] Two sets of sea surface temperature/sea ice changes are used to test the sensitivity of tracer transport to the pattern of warming in the doubled CO_2 climate. One set (2CO2WT) has greater tropical and high latitude sea surface temperature changes than the other (2CO2), although both fall within the range of plausible response. Simulations were done both with and without interactive ozone. Results show that the SST pattern affects the circulation change throughout the troposphere and middle atmosphere; the ozone interaction affects primarily the upper stratosphere, but through wave-mean flow interaction has effects that extend down into the upper troposphere. Both experiments feature increased tropospheric/stratospheric exchange at low latitudes and greater vertical mixing within the troposphere; only the WT experiments result in increased interhemispheric transport and a more direct circulation in the high latitude stratosphere. Ozone increases in the upper stratosphere and decreases in the lower stratosphere in all the simulations, with greater transport of high latitude ozone into the troposphere in the WT runs. At sea level there is a more positive phase of the Arctic Oscillation (AO)-type oscillation, and this is also true at 100 mbar, but there is no significance in the middle troposphere and the sign is different in the middle stratosphere. Many of these results differ from those generated in older versions of the GISS GCMAM despite the same SST forcing due to differences in control run characteristics, which has implications for model intercomparison experiments. *INDEX TERMS:* 0341 Atmospheric Composition and Structure: Middle atmosphere—constituent transport and chemistry (3334); 0368 Atmospheric Composition and Structure: Troposphere—constituent transport and chemistry; 1620 Global Change: Climate dynamics (3309); 3334 Meteorology and Atmospheric Dynamics: Middle atmosphere dynamics (0341, 0342); *KEYWORDS:* tracer transports and climate, stratosphere and climate change, climate change and ozone, future SSTs and tracer transports

Citation: Rind, D., J. Lerner, J. Perwitz, C. McLinden, and M. Prather, Sensitivity of tracer transports and stratospheric ozone to sea surface temperature patterns in the doubled CO_2 climate, *J. Geophys. Res.*, *107*(D24), 4800, doi:10.1029/2002JD002483, 2002.

1. Introduction

[2] The possibility of increased atmospheric CO_2 affecting atmospheric dynamics has many ramifications, including effects such as changes in the phase of the Arctic Oscillation (AO) [e.g., *Shindell et al.*, 1999; *Fyfe et al.*, 1999; *Monahan et al.*, 2000; *Perlwitz et al.*, 2000], and altered distributions of tropospheric and stratospheric trace gases. In a recent publication [*Rind et al.*, 2001], we investigated the impact of the doubled CO_2 climate on various tracer transports. In the doubled CO_2 climate change used in that experiment, the subtropical residual circulation intensified in the upper troposphere/lower stratosphere, increasing the rate of tropical transfer of tropospheric air mass and constituents into the stratosphere by about 30%. Transport from the stratosphere to troposphere at higher latitudes also increased as the high latitude residual circulation intensified, so that the stratospheric residence time of bomb ^{14}C decreased by about 11%. Within the troposphere, interhemispheric transport was reduced by 5% due to decreased Hadley Cell intensity; greater poleward transport occurred within the northern hemisphere due to eddy/Ferrel Cell changes; and greater vertical transport took place from low levels to the middle and upper troposphere via increased penetrating and overall convective mass fluxes.

0148-0227/02/2002JD002483$09.00

[3] In that publication, and in work by *Rind et al.* [2002], the generality of these doubled CO_2 results were assessed by comparing the meteorological changes in the latest simulation to those generated with different sea surface temperature changes [*Rind et al.*, 1990, 1998]. The two effects that were the most robust were the increase in the subtropical residual circulation, and the increase in penetrating convection to the upper troposphere, although the magnitude of their increase depended on the degree of tropical warming. Increases in transport from the surface to the middle troposphere depended on the convection parameterization, while changes in the Hadley circulation and the residual circulation in the polar stratosphere depended on the latitudinal distributions of sea surface temperature change. Hadley Cell changes with increasing CO_2 have been known to vary from model to model (e.g., *Dai et al.* [2001] with the NCAR CCM found the Hadley Cell weakened by 10% by 2090, *Ramstein et al.* [1998] with the LMD model also found a 10% weakening with doubled CO_2, while *Senior* [1995] found an increased Hadley cell with the Hadley Centre model run at 250 km resolution, and no change at 500 km resolution).

[4] These comparisons were based on the overt meteorological responses, and they did not explicitly calculate what the effect would be on the tracer transports themselves. Furthermore, the latest experiment had used a newer version of the GISS Global Climate/Middle Atmosphere Model (GCMAM), so model dependence could not be separated from the effect of different sea surface temperature patterns. These limitations are removed here, as we use two of the sea surface temperature/sea ice changes in the same (newer) version of the model with on-line tracers, and compare their effects directly.

[5] To the extent that altered depictions of tropospheric climate change produce different dynamical responses extending into the stratosphere, the effect of the doubled CO_2 climate on stratospheric ozone and its transport into the troposphere might also be different. Our previous investigations of the response of ozone to increased CO_2 [*Rind et al.*, 1998; *Shindell et al.*, 1998] all used the older version of the GCMAM [*Rind et al.*, 1988]; how would it differ with the newer model, and how would it depend on the sea surface temperature changes? Furthermore, the older approach did not allow the ozone changes to be advected, a limitation which precluded investigation of changes in stratospheric/tropospheric transport. These questions are addressed briefly in this paper, and more extensively in a companion paper (C.A. McLinden et al., manuscript in preparation, 2002) as the linearized ozone photochemistry scheme (LINOZ) [*McLinden et al.*, 2000], including online transports, is incorporated into these experiments.

[6] Finally, the resulting changes in ozone distributions themselves might alter atmospheric dynamics. That issue is investigated by running the doubled CO_2/LINOZ simulations in two ways. In the first, the model is run with a climatological ozone field for atmospheric radiation purposes, and in those experiments the on-line ozone is a passive tracer. In the second, we substitute the LINOZ-produced ozone values in the radiation routine, so the doubled CO_2 ozone changes interact with the climate. The complete set of experiments allows us to separate which features of the atmospheric and tracer transport response depend on the altered sea surface temperatures, and which are affected by the ozone response.

[7] Following the introduction and model/experiment description (section 2), the different foci of this paper are presented sequentially: meteorological effects of the different SSTs (section 3), the effect on tracer transports (section 4), and on ozone (section 5), followed by the dynamical influence of the interactive ozone response (section 6). In the discussion (section 7) we comment on which results depended on the SST field, and which were affected by the stratospheric ozone changes; we also include a discussion of potential inter-model differences by comparison to the results given by *Rind et al.* [1998, 2001]. A summary of the main results is given in the conclusions (section 8).

2. Model and Experiments

[8] The model used for these simulations is the GISS GCMAM, model II′ with some alterations. In previous studies, several specific model weaknesses were identified with the previous 31-layer version of the model [*Douglass et al.*, 1999; *Pawson et al.*, 2000]. Chief among these was a weaker than observed subtropical barrier to tracer transport in the stratosphere, insufficient vertical resolution in the lower stratosphere, reduced stratospheric winter variability, and reduced vertical transport to the upper stratosphere. In comparison to the previous version [e.g., *Pawson et al.*, 2000], the model now has 53 layers in the vertical, in conjunction with $4^\circ \times 5^\circ$ resolution. The increased vertical layering provides for 500 m resolution in the middle to upper troposphere, 0.5 to 1 km resolution in the lower stratosphere, sufficient to resolve important gradients in that region [*Douglass et al.*, 1999], and 2 to 2.5 km in the upper stratosphere. This layering can be compared with the 1.5 to 2 km resolution between 2 and 20 km used in the previous, 31-layer version of the model. The fourth order momentum scheme [*Rind and Lerner*, 1996] used in the 31-layer model was found to produce a tendency for spurious polar easterlies in the upper troposphere, which had the effect of limiting interannual variability, and also altering planetary wave refraction so as to reduce the stratospheric jet intensity. It is replaced in this model by a second order momentum scheme, which cured both of these problems. These changes also ameliorated the leakiness of the subtropical barrier, and the smaller than observed transport into the upper stratosphere. However, the problems still remain to some extent and may quantitatively affect the results; the mean age of air at 20 km varies from 1.5 years in the tropics to 3.5 years at 60°N, compared with 1 year in the tropics to 4 years at 60°N in observations [*Andrews et al.*, 2001].

[9] Although the second-order moments advection scheme [*Prather*, 1986] captures finer resolution effects than would be apparent from the given $4^\circ \times 5^\circ$ horizontal resolution, this coarse grid is not likely to capture the physical intricacies of stratosphere/troposphere exchange associated with fine-scale tropopause folds. Overall, the troposphere/stratospheric exchange is similar in this model to the previous $4^\circ \times 5^\circ$ versions of the stratospheric model, which were shown to be produce generally realistic magnitudes of transport [*Rind et al.*, 1999]. The model's large-scale and eddy processes appear to be producing overall

Table 1. Simulations Used in This Study

	SSTs/Sea Ice	Ozone
Control	current	noninteractive
Control (I)	current	interactive
$2CO_2$	*Rind et al.* [2001]	noninteractive
$2CO_2$ (I)	*Rind et al.* [2001]	interactive
$2CO_2$WT	*Rind et al.* [1998]	noninteractive
$2CO_2$WT(I)	*Rind et al.* [1998]	interactive

replicas of real-world processes without all the details; the climate change effect of such differences can only be gauged by future experiments with finer resolution models.

[10] For the doubled CO_2 experiments, we continue the approach used by *Rind et al.* [2001] and input altered sea surface temperature/sea ice fields from previous equilibrium experiments. The atmospheric CO_2 is doubled as well. The first set of experiments (called "2 CO_2") uses the same doubled CO_2 changes in sea surface temperatures as given by *Rind et al.* [2001], which were originally generated by a nine-layer version of the GISS model II′. The control runs and the experiments are run both with and without the ozone changes interacting with the radiation field (see Table 1). The second set of experiments uses the sea surface temperatures/sea ice field generated by an equilibrium run of the older version of the GISS GCMAM [*Rind et al.*, 1998]. In both cases, fixed dynamical ocean transport in conjunction with a mixed layer ocean (a "q-flux ocean") was used in the original simulations to allow the sea surface temperatures to change.

[11] The marine surface (sea surface plus sea ice) temperature differences for the individual experiments are shown in Figure 1, with the resulting surface air temperature changes (for the noninteractive experiments) shown in Figure 1b. Since the sea surface temperatures from *Rind et al.* [1998] featured a warmer tropical temperature response, experiments which used those values are called $2CO_2$ WT (for warmer tropics), although the runs also feature warmer high latitude temperatures.

[12] Which SST pattern is more realistic? The differences are largely associated with a change in the cloud cover parameterization and cloud feedbacks [*Rind et al.*, 2002]. The tropical warming in the two simulations in general varies between 2.5° and 4°C (Figure 1a). *Yao and Del Genio* [1999] show that such variations can be generated by differences in the parameterized cloud feedback within the range of current uncertainty. The smallest response occurs when thick anvil clouds arise in association with tropical convection (reducing solar insolation reaching the surface) and no cloud optical thickness feedback is allowed. The greatest warming occurs with the reverse situation: Optical thickness is predicted (and decreases in the tropics as climate warms due to water depletion by precipitation), while anvil clouds are not included. *Yao and Del Genio* [1999] argue that the optical thickness feedback is supported by observations, while the realism of the anvil detrainment feedback is more difficult to assess. That would suggest that a higher tropical sensitivity might be more realistic if one had to choose between the two, although numerous processes (including other cloud parameterizations) affect the overall and tropical sensitivity. At this point no conclusion can be definitive. The overall warming in $2CO_2$WT is slightly higher than the IPCC nominal range of 1.5°–4.5°C (as shown in Table 2).

[13] In addition to ozone, the other online tracers used were those discussed by *Rind et al.* [2001]: CO_2, SF_6, Rn^{222}, CFC-11, CH_4, N_2O, and bomb ^{14}C. The sources/sinks of each of these tracers is given by *Rind et al.* [2001]; the stratospheric photochemical sinks for CFC-11, CH_4 and N_2O were calculated in a consistent manner with the LINOZ photochemistry.

[14] The control runs and experiments were integrated for 12 years with results reported for 10 year averages. In addition, we investigated whether the differences seen during five years in the first half of the simulations were similar to those during the last half, and discuss only those which had consistent changes for the two time periods. A complete list of the control runs and doubled CO_2 simulations is given in Table 1.

3. Meteorological Effects of the Different Sea Surface Temperature Patterns

[15] The different sets of sea surface temperatures help generate different meteorological responses. We concentrate on those phenomena deemed responsible for changes in transports, and the dynamics discussion is focused on the Northern Hemisphere. To indicate the robustness of the conclusions, and/or the impact of the interactive ozone, we

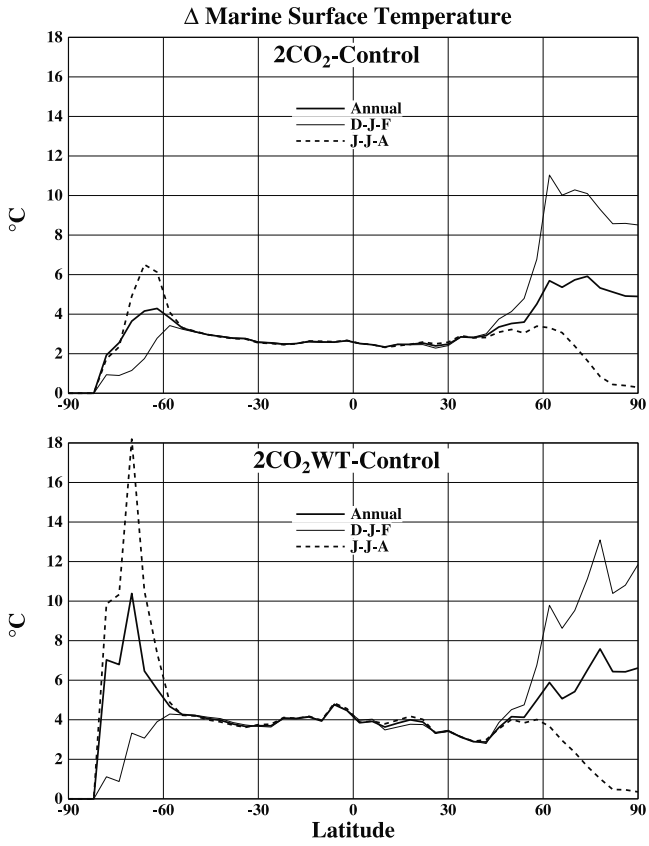

Figure 1a. The marine surface temperature (input sea surface temperature plus calculated sea ice temperature) anomaly in the two experiments ((top) $2CO_2$ and (bottom) $2CO_2$WT).

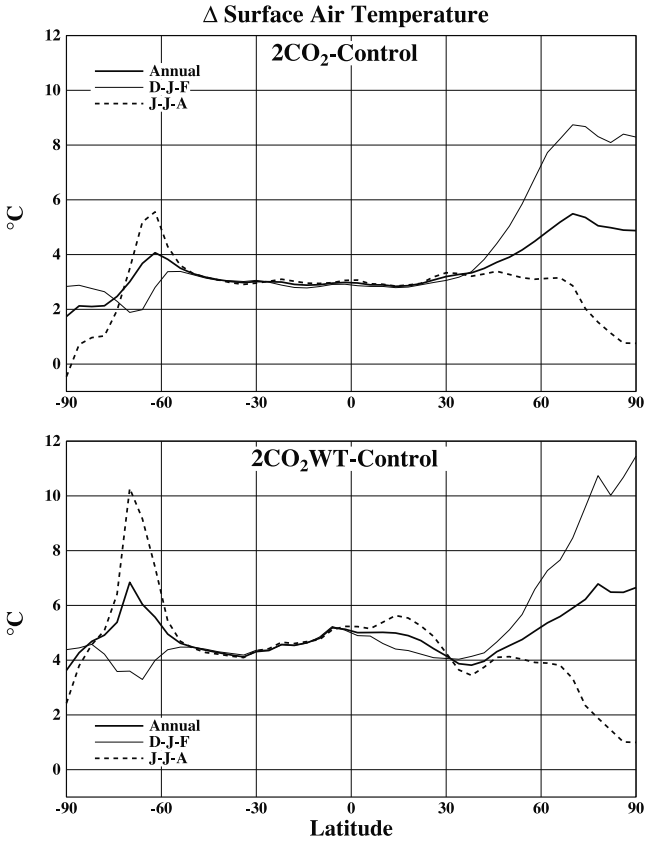

Figure 1b. As in Figure 1a except for surface air temperature changes calculated in the experiments.

often show results from both the noninteractive and interactive runs.

[16] Given in Table 2 are the annual, global average quantities of the relevant parameters (except for the peak stream function values, which are shown for the two solstice seasons). As an indication of the consistency of the results, we also show the average difference in the respective quantities over the two different 5-year periods (years 2–6 versus years 8–12). The $2CO_2$WT runs are considerably warmer than the $2CO_2$ simulations. The negative value of the net radiation at the model top for all the doubled CO_2 simulations show that had the sea surface temperatures been allowed to adjust, the runs would have cooled considerably. Given the magnitude of the imbalance, we estimate that this model has an equilibrium climate sensitivity for doubled CO_2 of about 2.65°C, or about 0.66°C/Wm^2.

[17] Of relevance for interhemispheric transport in the troposphere, the Hadley Cell during Northern Hemisphere winter is intensified in the $2CO_2$WT runs, with little change in $2CO_2$. Of relevance for intrahemispheric transport, planetary longwave energy increases substantially in the $2CO_2$WT runs, although eddy kinetic energy in general shows only small changes; again there is little change in either of these quantities in the $2CO_2$ simulations. Concerning vertical mixing within the troposphere, penetrative convective mass flux increases in all the doubled CO_2 simulations, more so in $2CO_2$WT, though total convective mass flux decreases somewhat in all the experiments, again more so in the WT runs. With increased penetrative convection, there is the possibility of reducing the time-averaged instability, decreasing more shallow convection.

[18] Shown in Figure 2 are the temperature changes in the different experiments, with tropospheric warming and stratospheric cooling as expected. The prime difference is that the WT experiments have greater warming in the tropical upper troposphere (and at the tropical tropopause), consistent with their warmer sea surface temperatures. In addition, the WT runs have greater warming at high latitudes during winter (Figure 1b). Given in Figures 3a and 3b are the resulting changes in zonal wind and Eliassen-Palm (EP) fluxes (the zonally averaged wave energy fluxes normalized by the zonal wind). The WT runs have greater relative west wind increases from 45°S to 45°N in the upper troposphere and lower stratosphere; over this range of latitudes, all of the doubled CO_2 simulations show relative equatorward propagation of EP fluxes in conjunction with these wind changes. At the highest latitudes, however, only $2CO_2$ shows west wind increases in the troposphere during Northern Hemisphere winter, as the greater warming in the WT runs leads to greater relative east winds, and poleward wave refraction. The decrease in high latitude temperature gradient imposed in WT at the surface (Figure 1b) extended up to some 6.5 km altitude, reducing the zonal wind shear throughout that region.

[19] The EP flux divergence changes for the different simulations are shown in Figure 4. Associated with the relative equatorward EP flux refraction change, increased convergence occurs in the lower stratosphere in both hemi-

Table 2. Annual Atmospheric Features in the Different Experiments

	Unit	Control	Control (I)	$2CO_2$	$2CO_2$ (I)	$2CO_2$ WT	$2CO_2$ WT(I)	5-Year Δ
Global surf temp	°C	12.39	12.35	15.67	15.67	17.13	17.11	0.007
Sea ice coverage	%	4.4	4.4	2.6	2.6	2.3	2.3	0
Air temperature	°C	−25.33	−25.30	−22.62	−22.55	−20.87	−20.87	0.013
Water vapor	mm	20.2	20.1	24.6	24.6	27.4	27.3	0.03
Cloud cover	%	68.8	68.7	66.3	66.2	65.3	65.1	0.03
Planetary albedo	%	32.33	32.27	30.28	30.39	30.18	30.30	0.08
Net radiation at model top	Wm^{-2}	−0.1	−0.4	−1.1	−1.5	−3.5	−3.9	0.016
Moist convective mass flux	10^9 Kgs^{-1}	1554	1568	1546	1550	1474	1483	1.5
Moist control mass flux at 195 mbar	10^9 Kgs^{-1}	141.3	145.5	222.8	232.0	278.7	290.0	0.6
Eddy kinetic energy	10^4 Jm^{-2}	64.9	65.0	63.5	64.2	67.2	67.5	0.27
EKE, wave numbers 1–4	10^{17} J	647	645	639	651	697	704	9.67
Peak D-F stream function	10^9 Kgs^{-1}	−175	−178	−173	−180	−208	−213	3
Peak J-A stream function	10^9 Kgs^{-1}	203	199	199	200	197	202	1.67

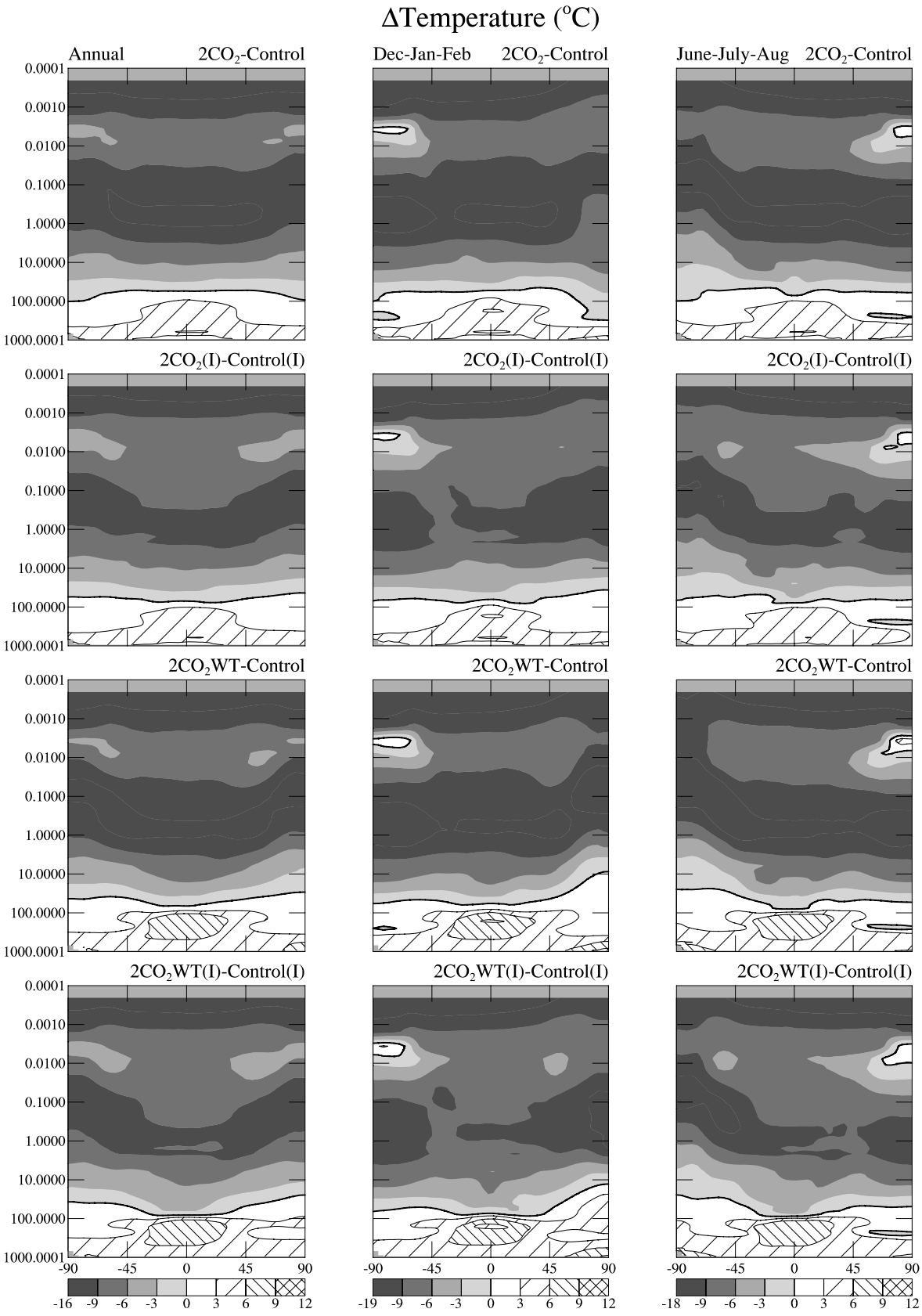

Figure 2. Temperature changes in the different experiments, averaged over the last 10 years. Shown are the results for the annual average and the two solstice seasons for (top) $2CO_2$, (second row) $2CO_2$(I), (third row) $2CO_2$WT and (fourth row) $2CO_2$WT(I).

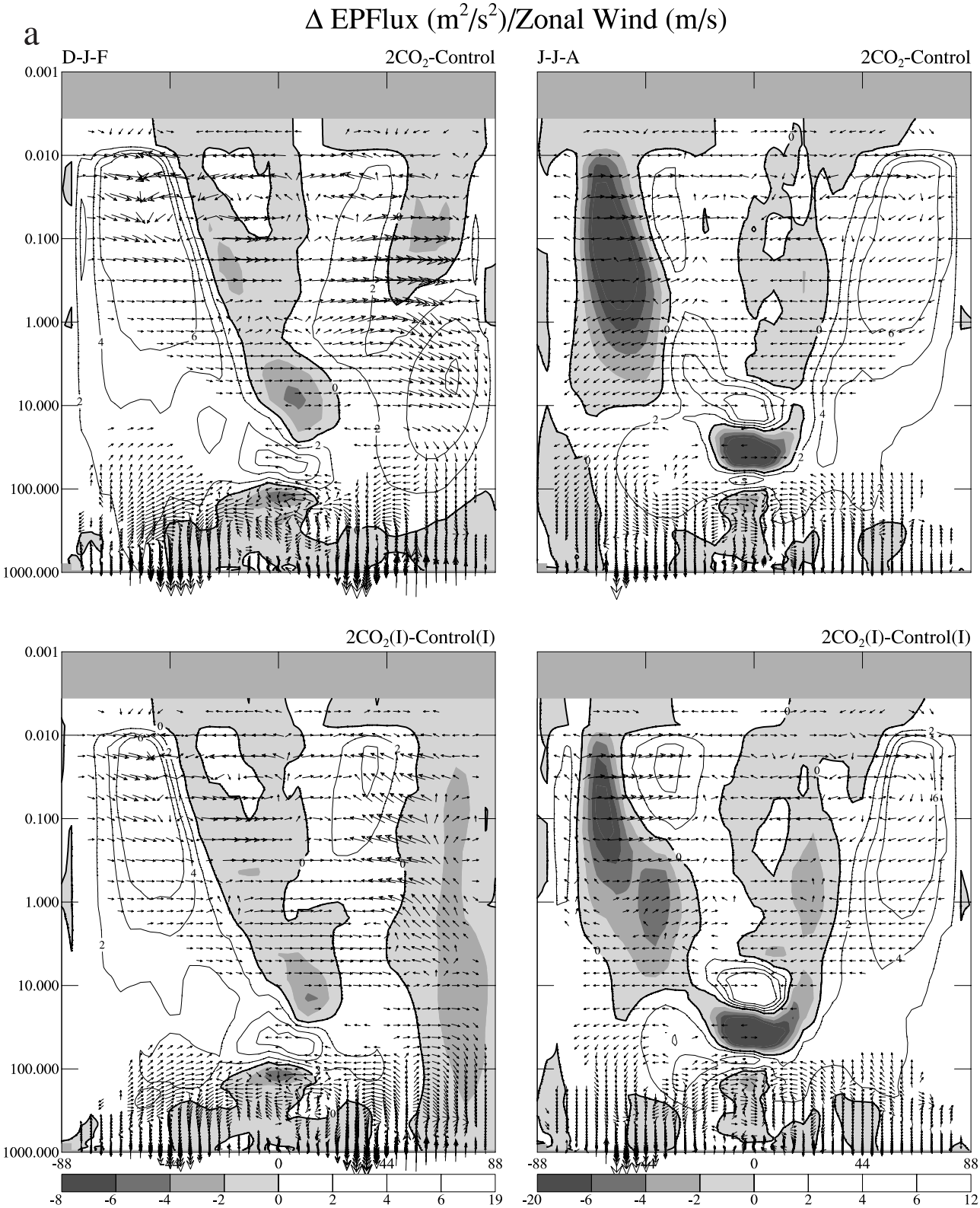

Figure 3. Change in the zonal winds (shading/contours) and EP fluxes (arrows) for the two solstice seasons in the different experiments (a) $2CO_2$ and $2CO_2$(I) and (b) $2CO_2$WT and $2CO_2$WT(I).

spheres from 45°S to 45°N, more so in the WT runs. In addition, the wind changes in the upper troposphere/lower stratosphere alter the wave refraction, and lead to greater EP flux convergences in the WT runs above 10 mbar primarily poleward of 45°N. In the extratropical troposphere, EP flux convergences are associated with the east wind change at the highest latitudes, while divergences arise with the west wind change at upper midlatitudes. These effects are also

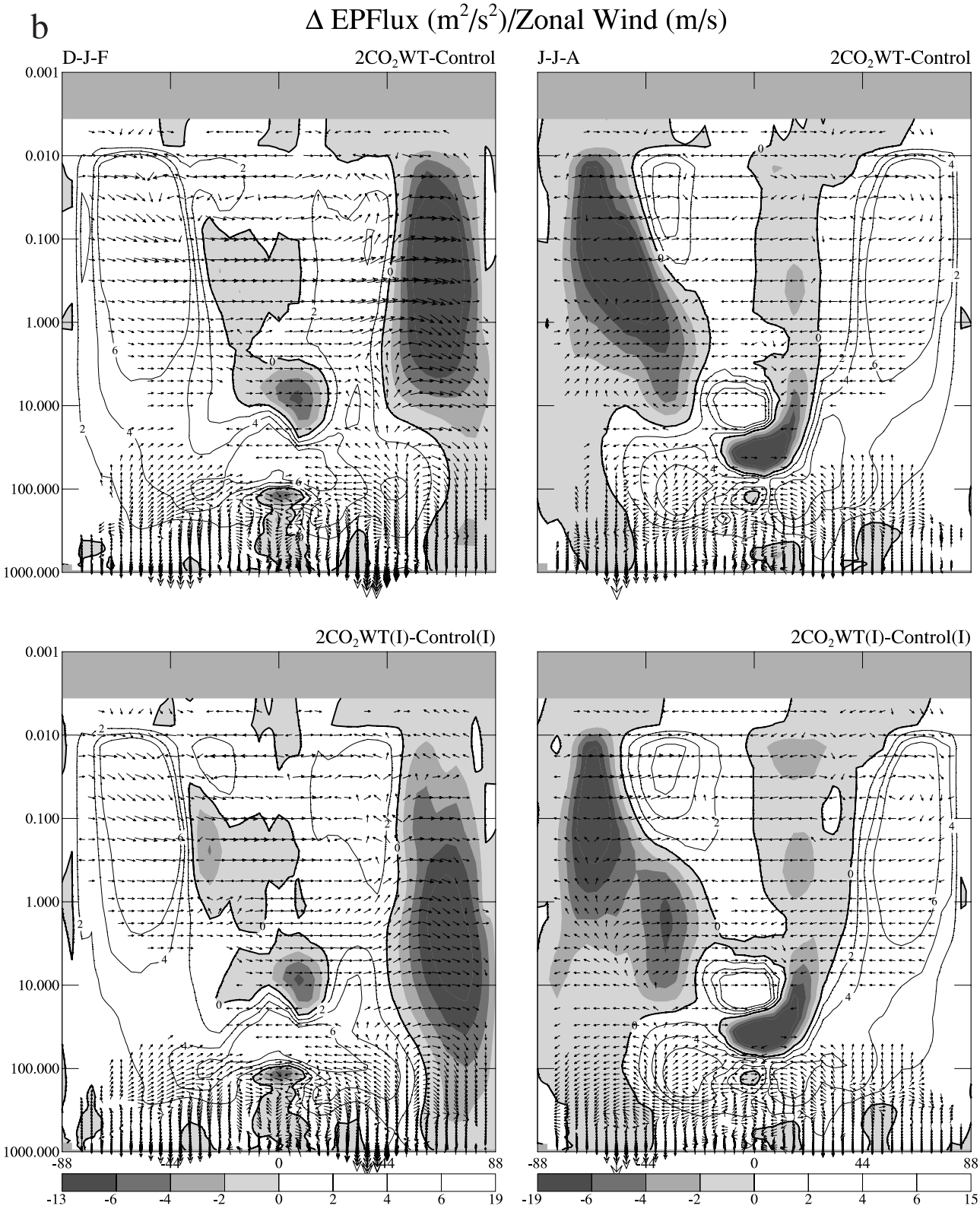

Figure 3. (continued)

greatest in the WT runs, and also somewhat larger in the interactive runs of each set.

[20] Changes in the transformed Eulerian (residual) circulation are presented in Figure 5. The intensified EP flux convergences drive an increased residual circulation at low latitudes in all the doubled CO_2 simulations, more so in the WT runs. At higher latitudes during Northern Hemisphere winter, the intensified EP flux convergences shown in Figure 4 above 10 mbar help the 2CO_2WT runs drive a more direct circulation from 10 to 100 mbar via the down-

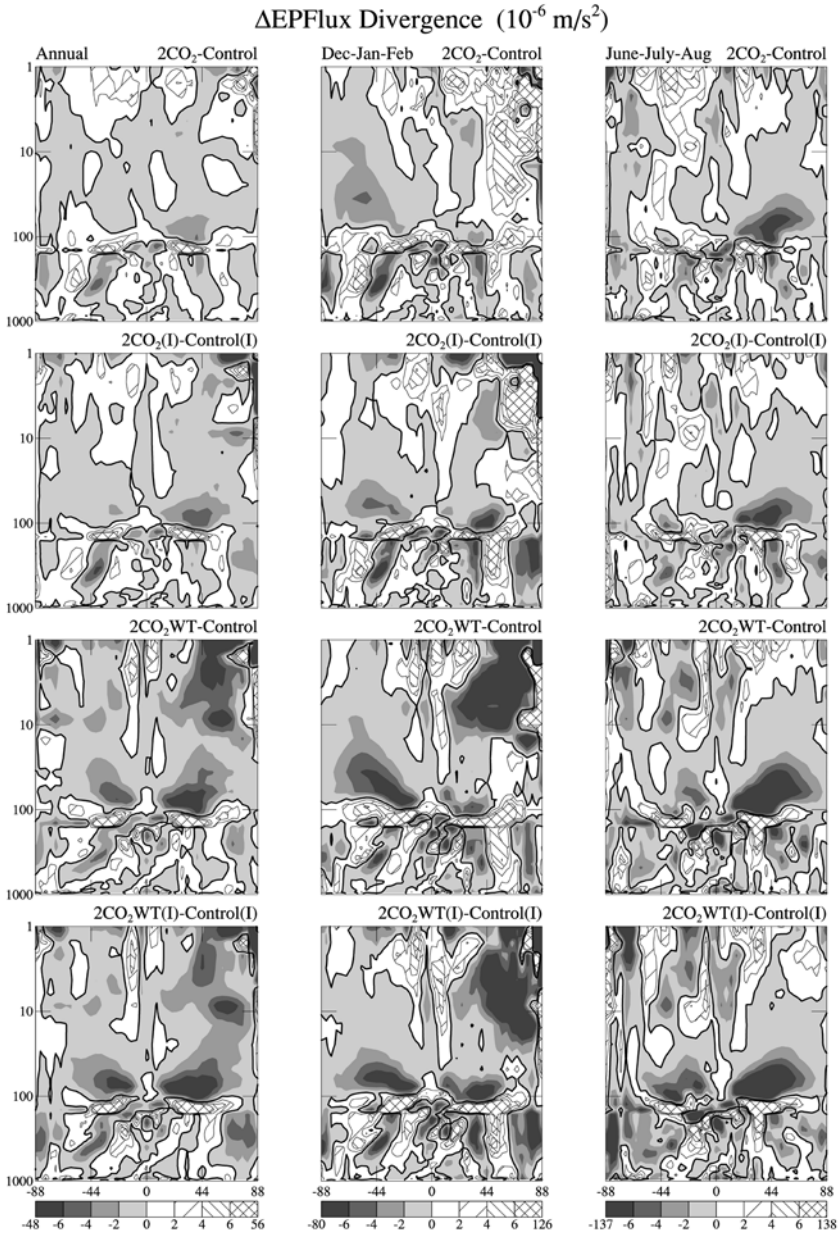

Figure 4. Change in the EP flux divergence in the different experiments.

ward control principle [*Haynes et al.*, 1991]. In contrast, the circulation is somewhat more indirect in the same region in $2CO_2$. In the troposphere, the more direct circulation at the highest latitudes follows the EP flux convergences, both being greatest in the WT simulations.

[21] These differences in high latitude response provide for a different pattern of geopotential response. The WT runs have increased 10 mbar heights around the pole in the winter hemisphere (Figure 6, left), while the $2CO_2$ runs have smaller changes or decreases. These results are consistent not only with the amount of high latitude warming, but also the EP flux convergence changes at high latitudes above 10 mbar with their generation of the residual circulation, i.e., EP flux convergence, a more direct circulation, and subsidence warming in the WT runs. From this perspective, the WT runs have a change toward the negative phase of the Arctic Oscillation (AO) (weaker polar vortex) in the midstratosphere, while in $2CO_2$ there is greater cyclonicity like the positive phase of the Arctic Oscillation.

[22] However, from the perspective of the sea level pressure (Figure 6, right) the results are very different. Now it appears qualitatively as if all the runs are producing the positive phase of the AO and North Atlantic Oscillation, the latter with lower pressure in the vicinity of the Icelandic Low, and relatively higher pressure near Portugal. This result illustrates that in a climate change situation one cannot necessarily expect the recent barotropic nature of AO response [*Thompson et al.*, 2000] to prevail. We return to this point in the discussion section.

4. Changes in Transports

[23] In this section, we present changes in the transports as discussed by *Rind et al.* [2001]. While $2CO_2$ uses the

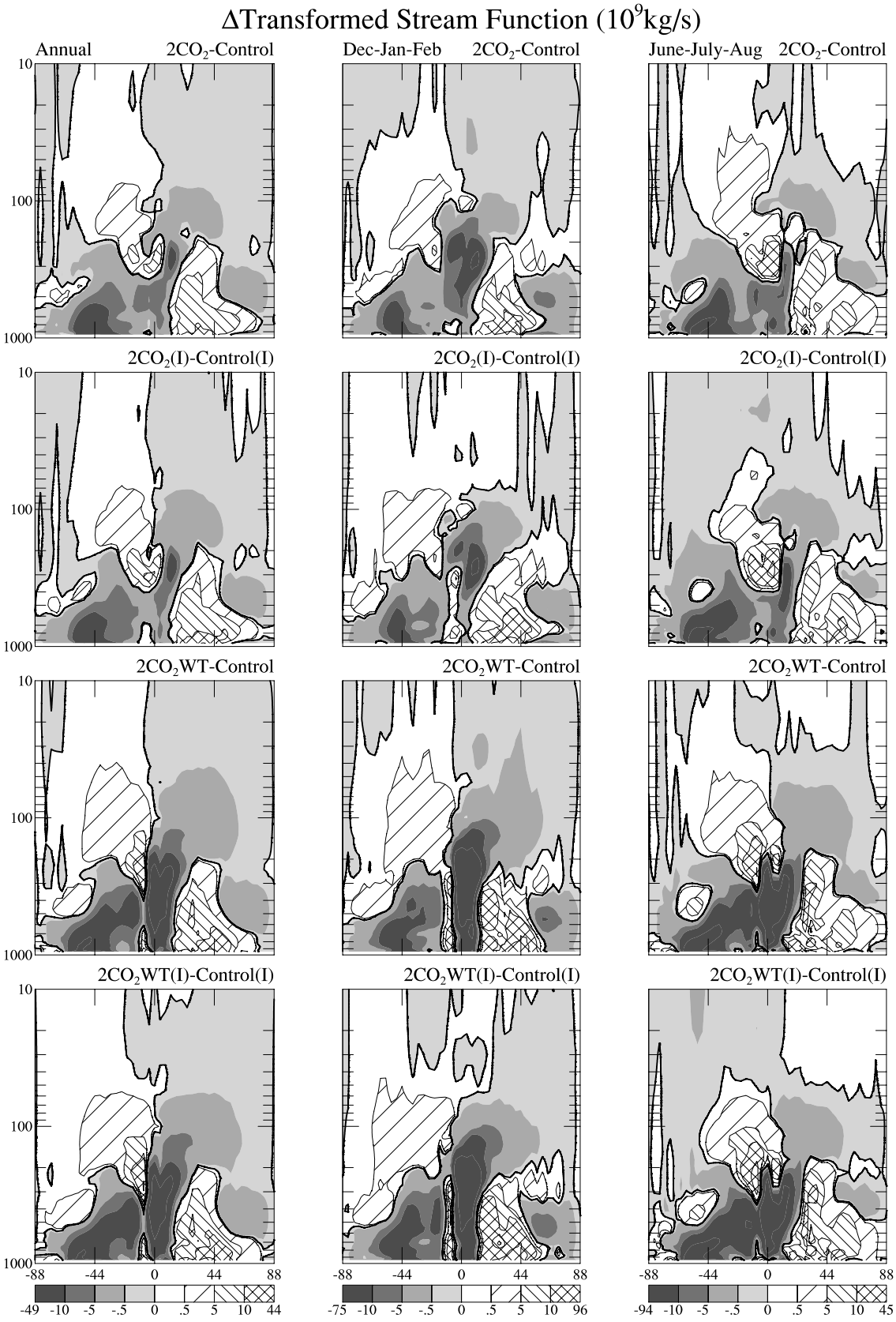

Figure 5. Change in the transformed Eulerian (residual) stream function in the different experiments. A positive value indicates a relative counterclockwise change, to a more indirect (direct) circulation in the Northern Hemisphere (Southern Hemisphere).

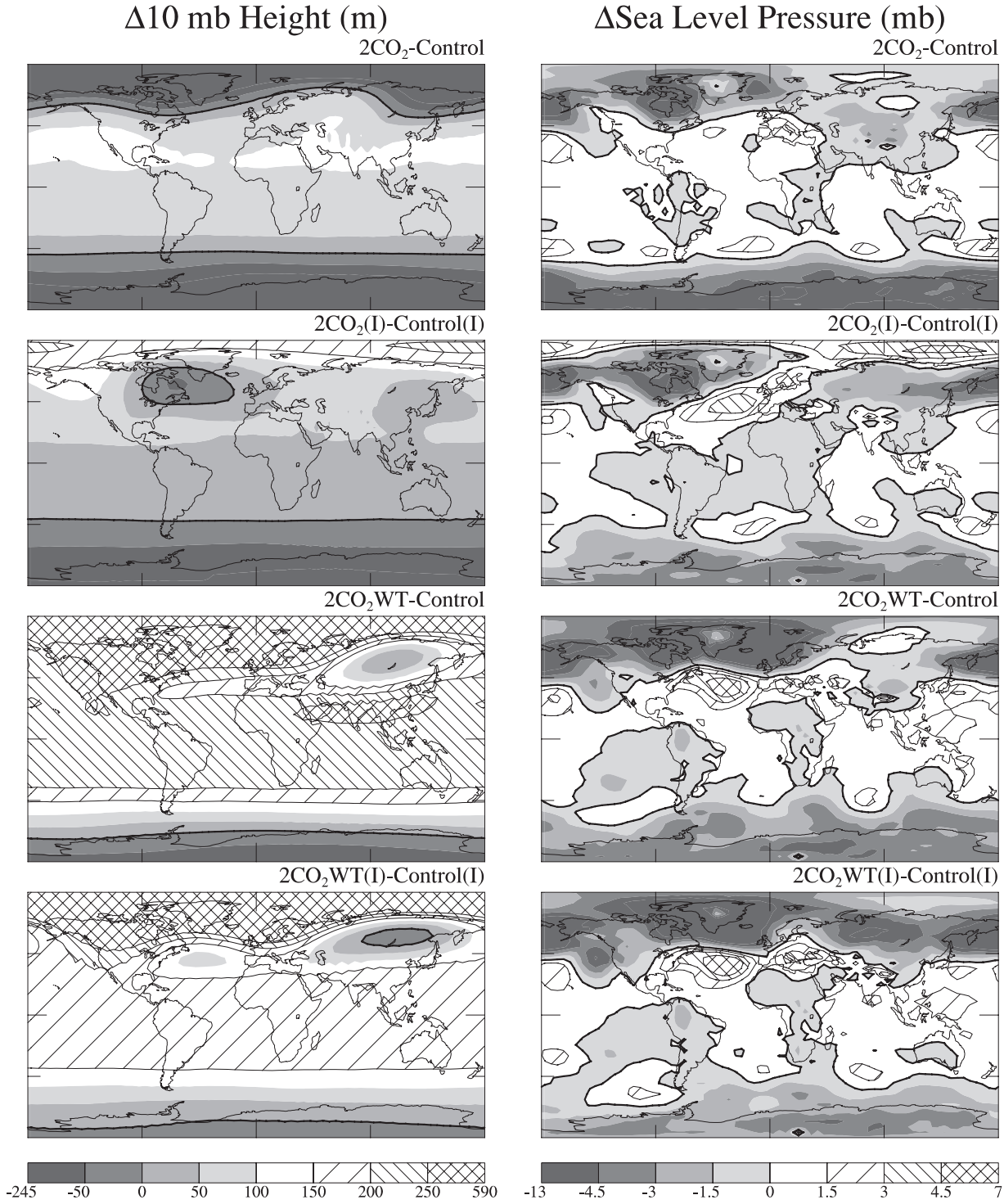

Figure 6. Change in the (left) 10-mbar heights and (right) sea level pressure for December–January–February.

same sea surface temperatures and sea ice changes as in that paper, this model has 53 layers (as compared to 31), and several of the physics routines (boundary layer, momentum advection, radiation) have been changed. The degree to which the boundary conditions can enforce the same response in these two related, but somewhat different models, will be addressed in the discussion section.

4.1. Interhemispheric Transport

[24] Given in Table 3 are the interhemispheric exchange times for three of the species in the different simulations, as well as the differences between the two five year time periods. There is little change in the 2CO$_2$ simulation, but interhemispheric exchange times decrease by 10–15% in 2CO$_2$WT. This is qualitatively consistent with the intensi-

Table 3. Interhemispheric Exchange Times (Years) in the Different Simulations

	SF_6	CFC-11	CH_4
Control	1.20	1.10	1.01
Control(I)	1.20	1.10	1.00
$2CO_2$	1.21	1.15	1.00
$2CO_2$(I)	1.20	1.13	1.00
$2CO_2$WT	1.07	0.97	0.89
$2CO_2$WT(I)	1.07	0.96	0.87
5-Year Δ	0.04	0.007	0.007

fied Hadley Cell during Northern Hemisphere winter (Table 2) in the WT experiments.

4.2. Intrahemispheric Transport

[25] For the same species shown in Table 3, there is greater southward transport within the Northern Hemisphere by a few percent (relative to the hemispheric tracer mass) in $2CO_2$WT, due both to the intensified Hadley Cell in Northern Hemisphere winter and the somewhat greater planetary longwave energy. There is little change in $2CO_2$.

4.3. Vertical Transport Within the Troposphere

[26] With respect to the distribution of short-lived species such as Rn^{222}, increased convection diminishes tropical gradients between low levels and the upper troposphere in all of the doubled CO_2 runs, and diminishes the gradients between the surface and midtroposphere in $2CO_2$WT (despite the overall decrease in convective mass flux indicated in Table 2). At high latitudes, the increased warmth provides for an additional radon source, from previously frozen ground, and results in increased vertical gradients away from the surface, more so in the warmer (WT) simulations.

4.4. Vertical Transport From the Troposphere to the Stratosphere

[27] The ratios of upward transport from 20°N to 20°S between experiment and control for levels in the upper troposphere and lower stratosphere are given in Tables 4a and 4b. In the $2CO_2$ runs, upward transport increases by 10–30% for all the species at all the levels, associated with the intensified residual circulation at these altitudes (Figure 5). The transport increases by even larger percentages in the $2CO_2$WT simulations.

[28] Also shown is the ratio of the global transports (in brackets), and the values are much lower than the tropical component. This is because the intensified tropical circulation cells lead to increased downward transport as well. Shown in Figure 7 is the change in vertical transport of CH_4 through 100 mbar for the four experiments; the other species show similar characteristics. The increased upward transport near the equator is apparent in all runs, greater with the WT simulations, while the increased downward transport in the subtropics is also evident. The global change is thus much less than the tropical upwelling component.

4.5. Vertical Transport From the Stratosphere to the Troposphere

[29] The change in the residual stream function shown in Figure 5 can be interpreted to imply that in all the doubled CO_2 simulations, there is increased downward transport through the Northern Hemisphere lowermost stratosphere at high latitudes and at midlatitudes (around 45°N) relative to the control run values (seen to some extent in Figure 7). To illustrate this more directly, given in Figure 8a is the change in SF_6 transport due to the large-scale dynamics (hence not including convection) for $2CO_2$; results for $2CO_2$WT given in Figure 8b show qualitatively similar features in the extratropics. The circulation change is especially effective for bomb ^{14}C which has its peak initial source around 50 mbar. Globally, downward transport increases by some 3–4% through 100 mbar, and by up to 10% through 240 mbar in the $2CO_2$WT experiments. This results in a shorter residence time for bomb ^{14}C in the stratosphere, with the effects greatest in the $2CO_2$WT runs; averaged over 6 years, there is 5.5% less ^{14}C in the atmosphere, with a decreased atmospheric residence time of 15–20%. Changes are smaller, but in the same direction, in the $2CO_2$ runs. As noted in the meteorology discussion, this in turn results from the greater relative EP flux convergences in the extratropics in driving a more direct circulation, especially in winter (Figure 5).

4.6. Transport Within the Stratosphere

[30] Evident in both Figures 8a and 8b is a two-cell distribution for the annual average change in the Northern Hemisphere stratosphere, with relative upwelling at the pole and equator, and downwelling around 45°N. Quantitatively the extratropical downwelling is greater in the WT runs as a result of the greater EP flux convergences above 10 mbar. The transport change is somewhat similar in the Southern Hemisphere except that the downwelling extends below 10 mbar only in the WT runs.

[31] The change in CH_4 distribution in the different runs is used to illustrate the effect of the altered circulation in Figure 9. Where air upwells, methane increases; regions of decrease in the Northern Hemisphere lower stratosphere and Southern Hemisphere middle stratosphere are associated with the relative downwelling. The stratospheric methane increase with greater flux from the troposphere is larger in the $2CO_2$WT experiments, which had the greater residual circulation change. Note that the increased interhemispheric transport in the troposphere (reduced Northern Hemisphere

Table 4a. Ratio of Vertical Transport Between $2CO_2$ and Control in the Tropics (20°N to 20°S) and Global (in Brackets)

Pressure, mbar	Run	CO_2	N_2O	CFC-11	CH_4	5-Year Δ
84	$2CO_2$	1.19 [1.03]	1.19 [1.11]	1.18 [1.12]	1.19 [1.10]	0.032 [0.04]
	$2CO_2$(I)	1.16 [1.01]	1.17 [1.07]	1.16 [1.10]	1.16 [1.06]	0.005 [0.05]
100	$2CO_2$	1.25 [1.03]	1.25 [1.11]	1.24 [1.11]	1.25 [1.09]	0.033 [0.04]
	$2CO_2$(I)	1.28 [1.02]	1.28 [1.07]	1.27 [1.09]	1.28 [1.05]	0.004 [0.05]
117	$2CO_2$	1.20 [1.02]	1.20 [1.11]	1.18 [1.10]	1.19 [1.08]	0.005 [0.13]
	$2CO_2$(I)	1.27 [0.99]	1.27 [1.07]	1.26 [1.08]	1.27 [1.03]	0.029 [0.05]
135	$2CO_2$	1.11 [0.97]	1.11 [1.12]	1.10 [1.08]	1.11 [1.06]	0.045 [0.04]
	$2CO_2$(I)	1.19 [0.95]	1.19 [1.08]	1.18 [1.06]	1.18 [1.00]	0.027 [0.06]

Table 4b. Ratio of Vertical Transport Between 2CO$_2$WT Experiments and Control in the Tropics (20°N to 20°S) and Global (in Brackets)

Pressure, mbar	Run	CO_2	N_2O	CFC-11	CH_4	5-Year Δ
84	2CO$_2$WT	1.55 [1.05]	1.55 [1.26]	1.52 [1.26]	1.54 [1.22]	0.060 [0.09]
	2CO$_2$WT(I)	1.56 [1.04]	1.56 [1.17]	1.55 [1.21]	1.56 [1.15]	0.035 [0.08]
100	2CO$_2$WT	1.74 [1.04]	1.74 [1.26]	1.69 [1.24]	1.73 [1.20]	0.036 [0.08]
	2CO$_2$WT(I)	1.82 [1.01]	1.83 [1.17]	1.79 1.19]	1.82 [1.12]	0.066 [0.04]
117	2CO$_2$WT	1.64 [0.96]	1.64 [1.26]	1.60 [1.22]	1.63 [1.15]	0.011 [0.08]
	2CO$_2$WT(I)	1.74 [0.92]	1.74 [1.17]	1.70 [1.16]	1.73 [1.07]	0.066 [0.07]
135	2CO$_2$WT	1.47 [0.87]	1.47 [1.26]	1.43 [1.19]	1.45 [1.05]	0.020 [0.06]
	2CO$_2$WT(I)	1.54 [0.83]	1.54 [1.17]	1.51 [1.14]	1.53 [0.97]	0.063 [0.07]

values relative to Southern Hemisphere) is also visible in the figure for the WT experiment.

5. Changes in Ozone Distribution

[32] The results presented in the previous section can be combined with the changes in ozone photochemistry to understand how ozone changed in these doubled CO_2 simulations. Shown in Figure 10 are the percentage changes in ozone on the annual average in the different experiments. Increases in the tropical upper stratosphere are associated with the colder temperatures due to doubled CO_2 and they do not depend on the different SST patterns, being similar in 2CO$_2$ and 2CO$_2$WT. The interactive runs have less ozone increase there, because as the ozone increases, the temperature does too, relatively, reducing the photochemical source. Therefore, in the upper stratosphere, while the ozone increase maximizes in the tropics in the noninteractive runs, the changes are of comparable value at low and high latitudes in the interactive simulations.

[33] Elsewhere, the SSTs do affect the ozone distribution. Ozone decreases in the tropical lower stratosphere, partly due to reduced UV penetration and chemistry, partly the result of increased tropical upwelling bringing up low tropospheric ozone concentrations (note that the only tropospheric ozone in these simulations is that which arises from stratospheric transport). This latter effect is greater with the warmer tropical SSTs. 2CO$_2$WT also features greater ozone increases at high latitudes and in the troposphere, due to its increased poleward and downward transport, as occurred for other species (e.g., methane, in Figure 9). The result is an increase in midtropospheric ozone from the stratospheric source in the 2CO$_2$WT simulations, and a decrease in the 2CO$_2$ runs (and for methane, with a tropospheric source, the result is just the opposite).

6. Dynamical Effect of Interactive Ozone

[34] The net effect of the greater tropical ozone increase in the noninteractive runs is to provide for warmer temperatures in the tropical upper stratosphere, by about 2°C. The warmer temperatures are then associated with a greater west wind increase in the subtropical stratosphere (e.g., see the 1 mbar wind change in Figures 3a and 3b); this affects the wave refraction and results in greater EP flux convergences (or smaller divergences) in the extratropical middle and upper stratosphere (e.g., between 10 and 1 mbar during Northern Hemisphere winter in Figure 4), and a more direct extratropical residual circulation in both winter hemispheres (Figure 5). This alteration in wave refraction pattern also produces greater EP flux divergences (or smaller convergences) at low latitudes in the middle and upper stratosphere (Figure 4), and thus affects the tropical residual circulation in the lower stratosphere and upper troposphere. Hence the increase in this circulation is slightly weaker in the noninteractive runs below 100 mbar, as can be seen from the tracer transports in Tables 4a and 4b. However, the downward transport is also weaker (Figure 7), and so the global transport upward is actually greater in the noninteractive runs (Tables 4a and 4b).

[35] In a related development, below about 30 mbar, and extending down through the middle troposphere, the interactive runs have greater EP flux convergences at high latitudes, greater relative east winds, and warmer temperatures during Northern Hemisphere winter (Figures 2–4). This effect is the result of their weaker subtropical west wind increase in the upper stratosphere diverting less wave energy upward, allowing for greater convergences below. This greater high latitude warming results in a greater increase in 10 mbar height at the pole (more negative phase of the AO) in the interactive runs (most obvious in Figure 6 for the 2CO$_2$ runs), an effect which extends down into the upper troposphere (see also Table 5, discussed below).

[36] We can summarize the results presented above by showing how the age of air changed in the various experiments (Figure 11), as deduced from the SF_6 tracer (as given by *Rind et al.* [2001]). The decrease in age of air throughout the stratosphere is greatest in the 2CO$_2$WT runs with their intensified residual circulation, and the decrease is greater in the noninteractive runs associated with their greater net global upward transport (Table 4, again not due to greater tropical upwelling). The noticeable increase in interhemispheric transport in the 2CO$_2$WT runs is evident in the troposphere as younger ages in the Southern Hemisphere,

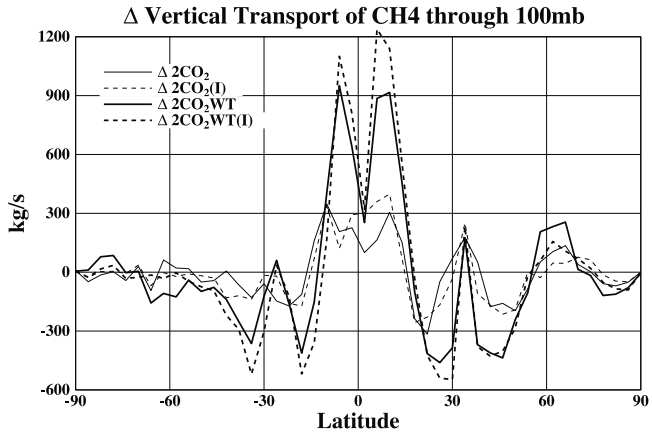

Figure 7. Change in annual vertical transport of CH_4 through 100 mbar in the different experiments.

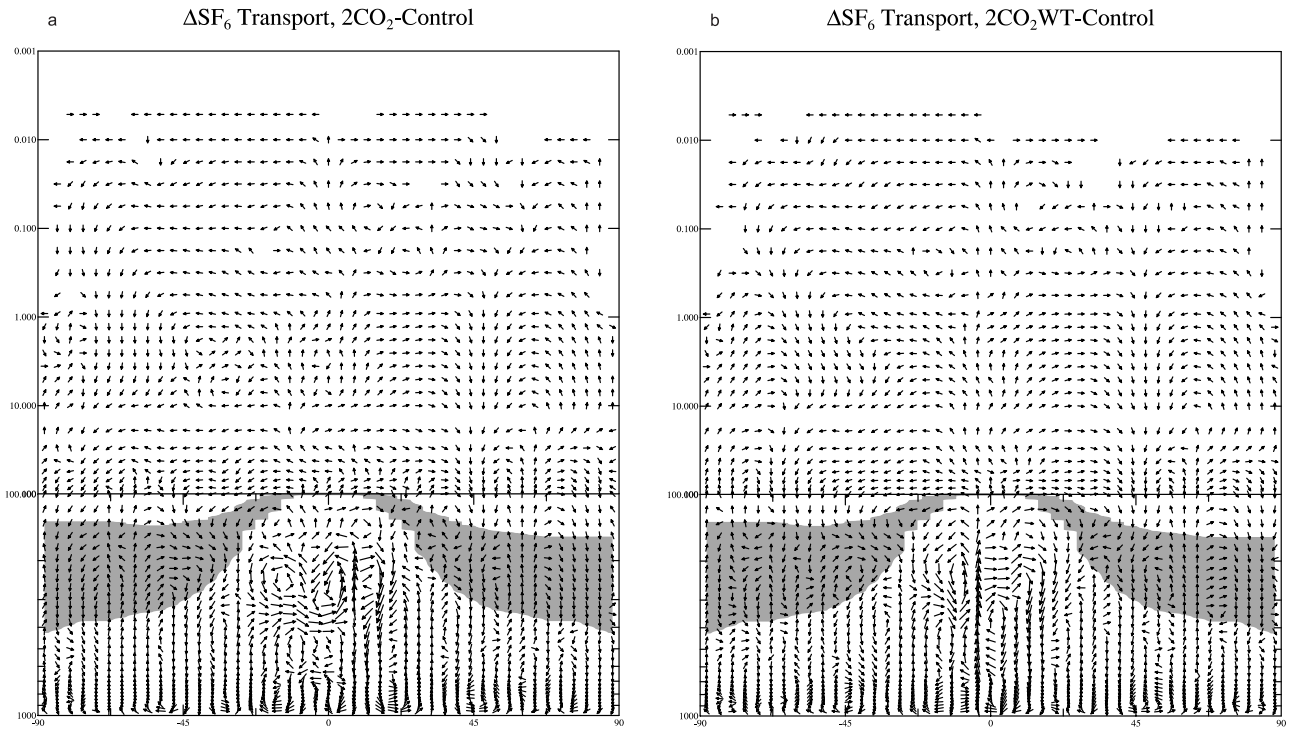

Figure 8. Schematic of the annual change in transport of SF_6 by the large-scale dynamics (not including convection) for (a) $2CO_2$ and (b) $2CO_2$WT. Shaded region indicates the lowermost stratosphere (potential temperature less than 380 K, and potential vorticity greater than 2×10^{-5} k mbar^{-1}s^{-1} outside the tropics and above 100 mbar in the tropics). To illustrate the altered pathways of tracer transport, all vectors are of unit length except in the tropical troposphere where the exceptionally large changes are shown as exaggerated arrows. Separate log pressure scales are used above and below 100 mbar for presentation purposes.

and to a lesser extent this appears to be true for portions of the troposphere in the $2CO_2$ runs as well, although that was not obvious from the hemispheric results given in Table 3. The difference relates to the increased age in the Southern Hemisphere tropical upper troposphere for the $2CO_2$ runs which, as can be seen from Figure 8a, is associated with an upper tropospheric vortex spanning the equator, with decreased age of air in the same region in the Northern Hemisphere. The effect is entirely missing in the $2CO_2$WT runs which have a coherent upward mass transport from low levels just south of the equator (Figure 8b). This distinction is related to the SST peak change south of the equator in the WT runs (Figure 1a). Greater downward transport from the stratosphere at extratropical northern latitudes in the $2CO_2$WT runs is indicated by the relative increase in age of air, especially relative to the strong decreases seen in the $2CO_2$ simulations.

7. Discussion

[37] In this section we discuss a number of issues raised by these results as well as some popular issues associated with the response to increasing CO_2 levels.

7.1. SST Versus Ozone Influence

[38] The range of experiments allows us to address the issue of what in the troposphere/middle atmosphere system is influenced by the SST patterns (the differences between the $2CO_2$ and $2CO_2$WT runs), and what is influenced by the ozone changes (the differences between the interactive and noninteractive runs).

[39] The SST pattern, in particular the degree of tropical warmth, affects the heating in the upper troposphere and its latitudinal temperature gradient, the winds in the upper troposphere and lower stratosphere, wave energy refraction and convergence in the stratosphere, and hence the circulation and winds throughout the middle atmosphere. Clearly, to know what will happen in the Middle Atmosphere we need to know the pattern of prospective SST change.

[40] The ozone response affects the magnitude of temperature change in the upper stratosphere, and the resulting latitudinal temperature gradient; this in turn affects wave energy propagation from the lower stratosphere, and wave energy convergences and circulation in the lower stratosphere, with effects which extend down into the upper troposphere. These dynamical responses illustrate how climate perturbations affecting the stratosphere can influence tropospheric processes due to wave-mean flow interactions. With respect to both the meteorology and the change in transports, the SST changes generally dominate the ozone influence, although the effects are comparable in some stratospheric regions.

7.2. Intermodel Differences

[41] A number of these results are consistent with expectations [*Rind et al.*, 2001, 2002]. The upper tropo-

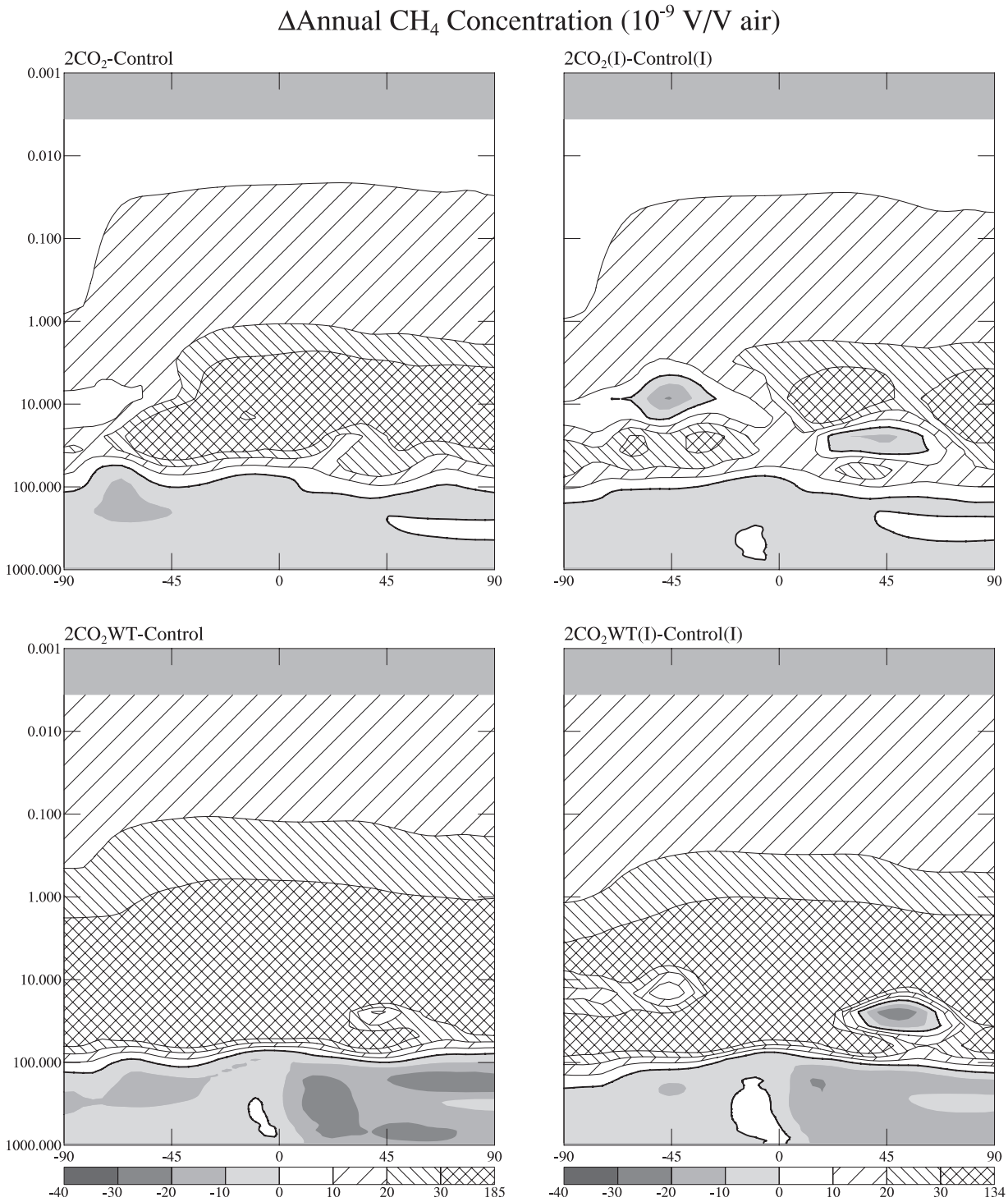

Figure 9. Change in annual average methane in the different experiments.

sphere/stratosphere tropical residual circulation did increase in both climate simulations, and the magnitude of increase was greater with warmer sea surface temperatures. These results were expected due to the influence of the tropical sea surface temperature warming on temperatures in the tropical upper troposphere, and the subsequent effect on west winds and planetary wave refraction at those altitudes. They support the assumption that increased transport from the troposphere to the stratosphere would be a robust result with different amounts of tropical warming. However, the tracer transport changes showed that the tropical upwelling is only part of the story, for the global increase in transport into the stratosphere is much less than the tropical change. The difference is associated with increased downwelling in the subtropics that accompanied the intensified tropical residual circula-

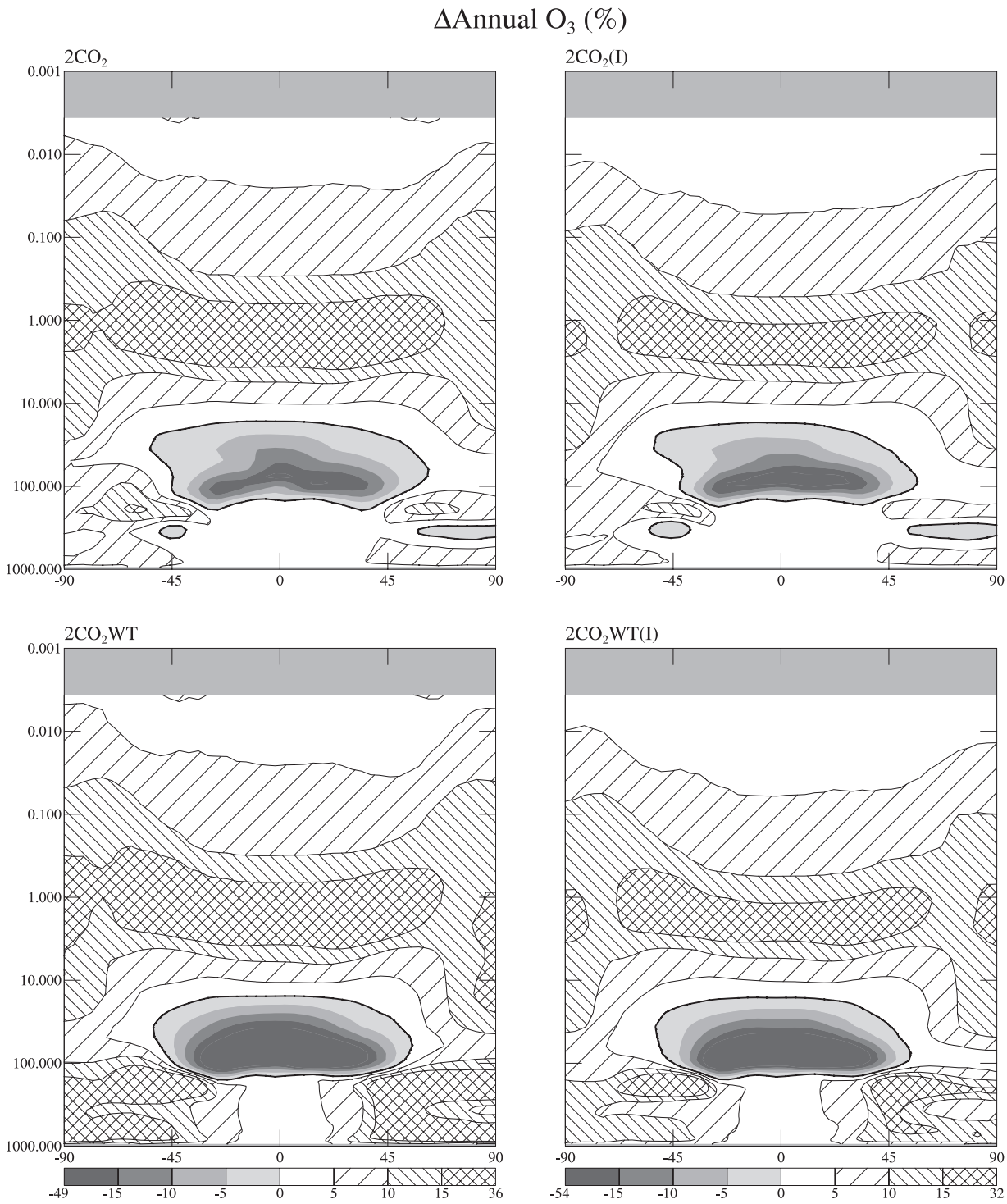

Figure 10. Change in annual average ozone (in percent) in the different experiments. Note that the tropospheric ozone and its change arises from stratospheric transport.

tion. This recycling of air within the 30°N to 30°S regime may be sensitive to the greater ''leakiness'' of the tropical pipe in the model compared to the real world.

[42] The Hadley Circulation response also matched expectations, at least in the sense that with the warmer tropical sea surface temperatures, the circulation would increase, and interhemispheric transport would become faster. The warmer tropical sea surface temperatures also led to a greater increase in penetrative convection and the corresponding increased transport of tracers to the upper troposphere, though that effect occurred in all the doubled CO_2 runs. And with greater tropical warming there was increased generation of planetary wave energy at the longest wavelengths, consistent with the increase in available

Table 5. AO-Type Responses During December–February[a]

		UNIT	$\Delta 2CO_2$	$\Delta 2CO_2$ (I)	$\Delta 2CO_2$WT	$\Delta 2CO_2$WT(I)
ΔSLP	32°N–52°N minus 60°N–80°N	mbar	2.28 (−1.14)	1.98	4.91[b] [3.88]	5.43[b]
Δ500 mbar Ht	32°N–52°N minus 60°N–80°N	m	−14 (−41)	−15	8 [−7]	9
Δ100 mbar Ht	32°N–52°N minus 60°N–80°N	m	76[c] (−19)	12	103[b] [142]	45[d]
Δ10 mbar Ht	32°N–52°N minus 60°N–80°N	m	196 (58)	−57	−96 [162]	−220[d]

[a]Results from *Rind et al.* [1998, 2001] are shown (without significance testing) in brackets or parentheses, respectively, for comparison.
[b]Significant at 99% level.
[c]Significant at 95% level.
[d]Significant at 90% level.

potential energy associated with hemispheric scales [*Rind et al.*, 1998].

[43] However, a number of the results were unexpected, relating primarily to changes associated with different versions of the GISS GCMAM. *Rind et al.* [2001] use the same marine boundary conditions as used in $2CO_2$ but with an earlier version of the model II′ GCMAM. In that simulation the Hadley Cell decreased in intensity, as did interhemispheric transport, by 5%; in contrast, in this $2CO_2$ experiment there were negligible changes in both quantities. Also, in the earlier simulation, total convective mass flux increased, as shown in Table 2, while this model produced a small decrease.

[44] The differing Hadley Cell response in the two models also likely influenced the high latitude response, by altering the magnitude of dynamical heat convergence in the midlatitude troposphere [*Rind et al.*, 2002]. Heating at this latitude, compared with heating at high latitudes, affects the latitudinal temperature gradient and zonal wind change in the upper troposphere, and hence planetary wave refraction. *Rind et al.* [2001, their Figure 3] show that the reduction in Hadley Cell intensity had minimized the midlatitude heating leading to decreased west winds in the upper troposphere at higher latitudes, relative poleward planetary wave refraction and higher sea level pressures at higher latitudes. In contrast, in the $2CO_2$ run here, during winter west winds increase at the higher latitudes in the upper troposphere, EP flux divergences occur and tropospheric subpolar lows are intensified. Why were these changes model dependent?

[45] We can address that question by comparing the current model to the version used by *Rind et al.* [2001]. The intermodel differences include the greater vertical resolution in the current model, both in the boundary layer (6 layers to 4 in the first 200 mbar) and overall (53 layers to 31 layers), and alterations in the model code, primarily in the boundary layer. To determine which component of the model changes affected each of the different results, we ran a control run version with reduced boundary layer and vertical resolution but with the newer 53-layer model code.

[46] The results showed that increasing the vertical resolution, including that in the boundary layer, reduced the latent heat and total surface fluxes, and with it the precipitation. Changes in the model code resulted in the newer model having weaker surface winds and often weaker eddy mixing in the boundary layer under unstable conditions. Increased vertical resolution resulted in greater amounts of penetrating convection to high levels and decreased fluxes to low levels.

[47] The control run differences provide explanations for the intermodel differences noted above. The newer version of the model is somewhat less sensitive to SST patterns, with weaker surface winds, surface fluxes and resulting precipitation; hence it responded more weakly to the altered SST fields it was given (e.g., no Hadley Cell change). The newer model also had greater penetrative convection relative to convection at other levels, so when climate warmed, and the penetrative convection increased, it was easier to stabilize the atmosphere and reduce convection in general. Furthermore with the greater increase in penetrating convection in the newer model, warming of the upper troposphere was greater; combined with the unchanged Hadley circulation this resulted in a greater latitudinal temperature gradient, stronger west wind increases and a more positive AO phase (discussed further below). The tendency of climate change simulations to mimic characteristics of the control run has been noted previously [*Mitchell et al.*, 1987; *Rind*, 1988; *Senior*, 1995].

[48] The $2CO_2$WT experiment should have produced simulations that resembled the results discussed by *Rind et al.* [1998] with the coarser resolution model, given that the sea surface temperature/sea ice changes of that run (from model II) were used in this one. The GCMAM II′ model has weaker convective fluxes due to reduced mass associated with each convective event, and hence the warming in the tropical upper troposphere is about 25% less than it was in the previous model. Consequently, the zonal wind increase in the upper troposphere is not as strong, and the magnitude of the wave refraction, EP flux divergence and residual circulation changes are somewhat reduced, but the overall pattern is similar. However, the AO phase changes differ with altitude, as discussed below.

[49] Given these intermodel differences for their current climate simulation, it would be reasonable to have the most confidence in those simulations that produce the most realistic current depictions. The reduced convective fluxes in GCMAM II′ are likely to be more realistic than the excessive values of the coarse grid model as deduced from radon distributions (at least in comparison to other models' radon results [*Rind and Lerner*, 1996]). Hence in that respect (although not with respect to sensitivity to SSTs) $2CO_2$WT should be given preference over the results from *Rind et al.* [1998]. The weaker surface response of $2CO_2$ is not necessarily an improvement, for example, the surface winds in the model were already too weak (as deduced from modeled soil dust [*Tegen and Miller*, 1998]). Hence the conclusions from $2CO_2$ are not necessarily to be preferred over those given by *Rind et al.* [2001] where they differ.

[50] The interactive ozone changes calculated by *Rind et al.* [1998], with the ozone anomaly scheme described by *Shindell et al.* [1998] that did not include ozone advection, peaked at 12% in the tropical stratopause region. In the

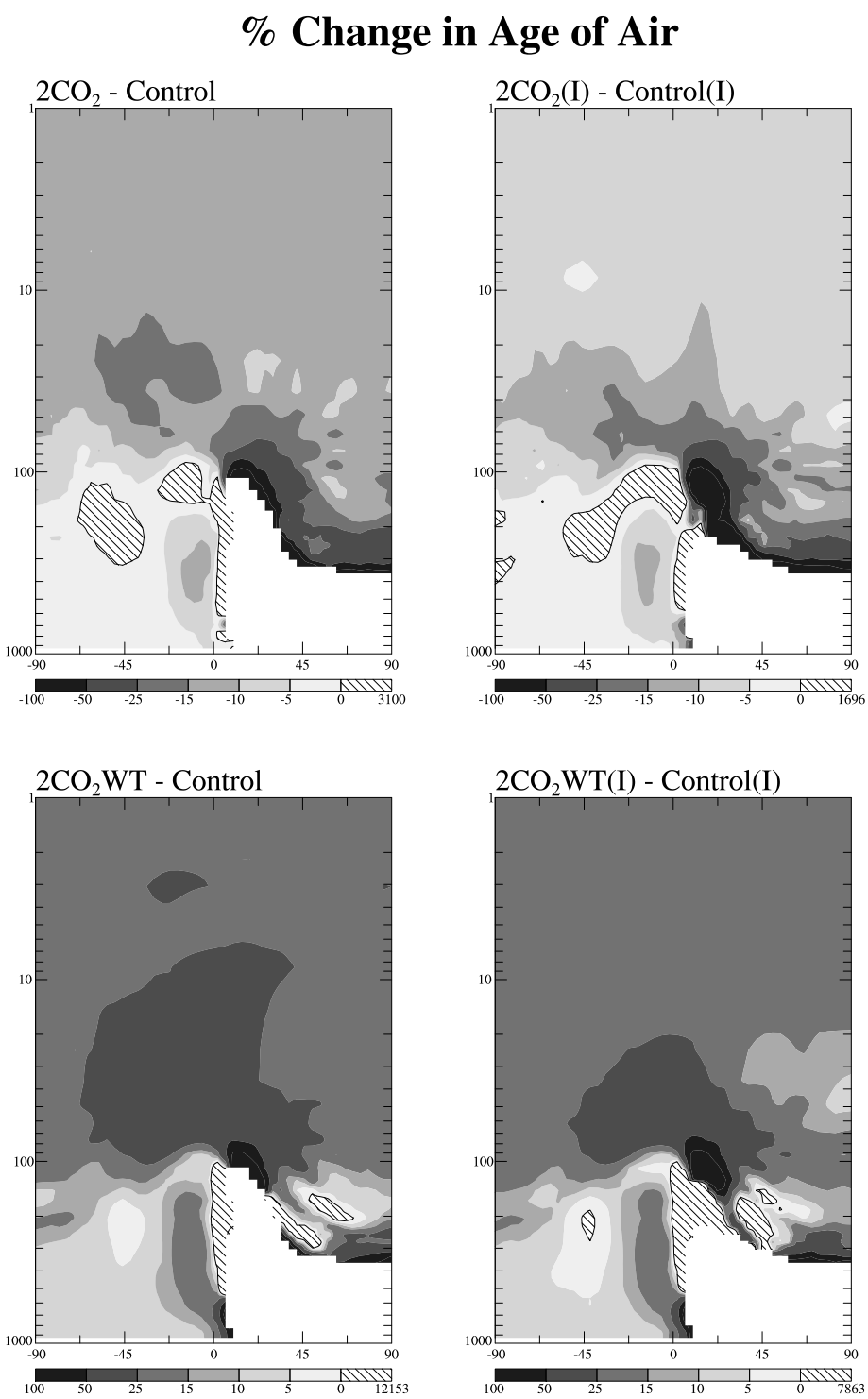

Figure 11. Percentage change in age of air in the various experiments as calculated from the SF_6 surface concentrations.

$2CO_2$WT simulations, the values are larger than that, with tropical stratopause peak values of 15–20%, perhaps due to the different ozone photochemical code. The ozone loss in the tropical lower stratosphere is 5–10 times larger in the new run, undoubtedly influenced by the ozone advection, with the intensified upwelling exaggerating the lower stratosphere loss. High latitude ozone gains are also larger when ozone advection is included. The radiative impact on the temperature structure of these ozone differences produces some additional cooling in the tropical lower stratosphere and slightly greater warming at high latitudes.

7.3. AO Changes

[51] Many, but not all model simulations have shown an increased positive AO phase with increasing atmospheric CO_2 [*Shindell et al.*, 1999; *Paeth et al.*, 1999; *Zorita and*

Gonzalez-Rouco, 2000; *Gillett et al.*, 2002a]. All the simulations shown here have decreased high latitude sea level pressures as well, as is evident in Figure 6. To assess whether these changes correspond to an altered phase of the Arctic Oscillation, we show in Table 5 the differences in sea level pressure or geopotential heights between approximately 30°N–50°N and 60°N–80°N (characteristic of the AO sea level pressure gradient), along with the significance of the results using a two-tailed T-test on the interannual variation for 10 modeled years. With the warmer tropical sea surface temperatures, at sea level a change to the positive phase of the AO-type oscillation is significant, and this is also true at 100 mbar, but there is no significance in the middle troposphere, and the sign is different in the middle stratosphere.

[52] The pattern of the EP flux change in all the experiments features significant tropospheric divergences at upper middle latitudes (providing a west wind acceleration), with convergences at high latitudes (for an east wind acceleration), as in Figures 3 and 4. This wind change is realized with lower pressure circa 70°N.

[53] The increased positive phase alters sign by the middle stratosphere in 2CO$_2$WT, which then features a weaker polar vortex (see also Figure 6), a result also found by *Butchart et al.* [2000] and *Gillett et al.* [2002b]. We also show in Table 5 (in brackets) the results from the previous simulation with these SSTs in the coarse grid model, in which the phase remained positive in the middle stratosphere; that is, the polar vortex was stronger. As can be seen in Figure 2, the temperature change in 2CO$_2$WT at high northern latitudes in the lower stratosphere exceeds that in the middle troposphere, and also exceeds that at midlatitudes, helping to change the phase of the AO. In contrast, the older model did not have such amplified warming in the polar lower stratosphere, and the positive AO phase change was maintained into the stratosphere (i.e., a more barotropic response). This temperature difference is consistent with the zonal wind change, which in the current simulations features weaker west winds at high latitudes, with relative poleward wave refraction, while the older model had stronger west winds and relative equatorward wave refraction at most high latitudes [*Rind et al.*, 1998, Figure 5]. The greater convective fluxes and tropical response in the older model led to greater energy convergence from the Hadley Cell change at lower midlatitudes in the upper troposphere, helping to produce these differences.

[54] We can also compare the results from the earlier version of the current model (shown in parentheses in Table 5) [*Rind et al.*, 2001] to the 2CO$_2$ results. The earlier model featured a relative negative AO phase in the sea level pressure field and throughout the troposphere, in contrast to the newer run with the same SST field. This model difference is also influenced by the different Hadley Cell convergences at midlatitudes, as discussed earlier in this section.

7.4. Stratospheric Water Vapor Change

[55] Given the increase in fluxes of tropospheric species into the stratosphere, as symbolized by the methane changes shown in Figure 8, one might have expected that (nonmethane) stratospheric water vapor values would have increased as well. In addition to the transport change, tropical zonal and time-averaged tropopause temperatures increased by 3°–4°C in the 2CO$_2$ experiments, and 4°–6°C in the 2CO$_2$WT experiments. At 164 mbar in the tropics specific humidity increased by 9%, in the 2CO$_2$ runs and increased by 45% in 2CO$_2$WT. Nevertheless, colder temperatures just above the averaged tropopause associated with the increased vertical velocities and localized penetrating convection enhanced condensation, removing all the excess moisture and more. Specific humidity decreased throughout the stratosphere, with reductions of greater than 20% between 100 and 30 mbar.

8. Conclusions

[56] Model simulations with doubled atmospheric CO$_2$ and two sets of sea surface temperatures (2CO$_2$ and 2CO$_2$WT) were used in GCM simulations with eight online tracers. Also included was a linearized ozone photochemistry run both interactively (I) and noninteractively with the radiation. The primary results from these experiments are summarized as follows:

- The simulations with the greater increase in tropical sea surface temperatures (2CO$_2$WT, 2CO$_2$WT (I)) caused an amplified tropical residual circulation response, including increased interhemispheric transport and an exaggerated increase in transport out of the tropical troposphere into the stratosphere. In the other simulations (2CO$_2$, 2CO$_2$(I)) interhemispheric transport did not change, and the increase in transport out of the tropical troposphere was smaller.
- At high latitudes, zonal winds become more easterly in the WT runs due to a combination of greater surface warming and increased EP flux convergences in the stratosphere. These effects are weaker or missing entirely in the other simulations.
- In all of the doubled CO$_2$ simulations, there is a more direct circulation at lower latitudes, a more indirect circulation at midlatitudes in the troposphere and higher latitudes in the stratosphere, and a more direct circulation at high latitudes in the troposphere and lower stratosphere. All of these circulation changes are greater in the WT experiments.
- Ozone increases in the upper stratosphere and decreases in the lower stratosphere in all of the doubled CO$_2$ simulations. In the WT experiments ozone increases at high latitudes as well, an effect which extends down into the troposphere, while the other simulations show decreases in high latitude ozone in the midtroposphere.
- The interactive runs show the smallest ozone increase in the tropics, as warmer temperatures reduce photochemical production. By altering the ozone gradients, the interactive runs alter the temperature gradients, winds and refractive properties of planetary waves, with some effect on the circulation extending down into the troposphere.
- At sea level there is a change to the positive phase of the AO-type oscillation and this is also true at 100 mbar, but there is no significance in the middle troposphere, and the sign is different in the middle stratosphere.
- Many of these results differ from those generated in older versions of the GISS GCMAM despite the same SST forcing, due to differences in control run characteristics.

[57] This last conclusion has implications concerning the use of altered sea surface temperatures in different GCMs as part of intercomparison projects. The two marine sur-

face data sets applied to the GCMAM were also made available to the GRIPS (GCM Reality Intercomparison Project) [*Pawson et al.*, 2000] so that different stratospheric modeling groups could run doubled CO_2 experiments with the same climate forcing. The goal of the project is, in effect, to compare how important intermodel differences are relative to the sea surface temperature forcings. The results presented in this paper, when compared with those from our earlier simulations, imply that intermodel differences outweigh the sea surface temperature forcings for a number of the features, and this is from a comparison of old and new GISS GCMs. We might expect the differences to be equivalent or larger among the modeling groups in general.

[58] **Acknowledgments.** This work was funded by the NASA ACMAP and EOS programs.

References

Andrews, A. E., et al., Mean ages of stratospheric air derived from in situ observations of CO_2, CH_4, and N_2O, *J. Geophys. Res.*, *106*, 32,295–32,314, 2001.

Butchart, N., J. Austin, J. R. Knight, A. A. Scaife, and M. L. Gallani, The response of the stratospheric climate to projected changes in the concentrations of well-mixed greenhouse gases from 1992 to 2051, *J. Clim.*, *13*, 2142–2159, 2000.

Dai, A., T. M. L. Wigley, B. A. Boville, J. T. Kiehl, and L. E. Buja, Climates of the twentieth and twenty-first centuries simulated by the NCAR climate system model, *J. Clim.*, *14*, 485–519, 2001.

Douglass, A. R., M. J. Prather, T. M. Hall, S. E. Strahan, P. J. Rasch, L. C. Sparling, L. Coy, and J. M. Rodriguez, Choosing meteorological input for the global modeling initiative assessment of high-speed aircraft, *J. Geophys. Res.*, *104*, 27,545–27,564, 1999.

Fyfe, J. C., G. J. Boer, and G. M. Flato, The Arctic and Antarctic oscillations and their projected changes under global warming, *Geophys. Res. Lett.*, *26*, 1601–1604, 1999.

Gillett, N. P., M. R. Allen, R. E. McDonald, C. A. Senior, D. T. Shindell, and G. A. Schmidt, How linear is the Arctic Oscillation response to greenhouse gases?, *J. Geophys. Res.*, *107*, 4022, doi:10.1029/2001JD000589, 2002a.

Gillett, N. P., M. R. Allen, and K. D. Williams, The role of stratospheric resolution in simulating the Arctic Oscillation response to greenhouse gases, *Geophys. Res. Lett.*, *29*, 1500, doi:10.1029/2001GL014444, 2002b.

Haynes, P. H., C. J. Marks, M. E. McIntyre, T. G. Shepherd, and K. P. Shine, On the "downward control" of extratropical diabatic circulations by eddy-induced mean zonal forces, *J. Atmos. Sci.*, *48*, 651–678, 1991.

McLinden, C. A., S. C. Olsen, B. Hannegan, O. Wild, M. J. Prather, and J. Sundet, Stratospheric ozone in 3-D models: A simple chemistry and the cross-tropopause flux, *J. Geophys. Res.*, *105*, 14,653–14,665, 2000.

Mitchell, J. F. B., C. A. Wilson, and W. M. Cunnington, On CO_2 climate sensitivity and model dependence of results, *Q. J. R. Meteorol. Soc.*, *113*, 293–322, 1987.

Monahan, A. H., J. C. Fyfe, and G. M. Flato, A regime view of Northern Hemisphere atmospheric variability and change under global warming, *Geophys. Res. Lett.*, *27*, 1139–1142, 2000.

Paeth, H., A. Hense, R. Glowienka-Hense, S. Voss, and U. Cubasch, The North Atlantic Oscillation as an indicator for greenhouse-gas induced regional climate change, *Clim. Dyn.*, *15*, 953–960, 1999.

Pawson, S., et al., The GCM-Reality Intercomparison Project for SPARC (GRIPS): Scientific issues and initial results, *Bull. Am. Meteorol. Soc.*, *81*, 781–796, 2000.

Perlwitz, J., H. F. Graf, and R. Voss, The leading variability mode of the coupled troposphere-stratosphere winter circulation in different climate regimes, *J. Geophys. Res.*, *105*, 6915–6926, 2000.

Prather, M., Numerical advection by conservation of second-order moments, *J. Geophys. Res.*, *91*, 6671–6681, 1986.

Ramstein, G., Y. Serafini-Le Treut, H. Le Treut, M. Forichon, and S. Joussaume, Cloud processes associated with past and future climate changes, *Clim. Dyn.*, *14*, 233–247, 1998.

Rind, D., Dependence of warm and cold climate depiction on climate model resolution, *J. Clim.*, *1*, 965–997, 1988.

Rind, D., and J. Lerner, The use of on-line tracers as a diagnostic tool in GCM model development, *J. Geophys. Res.*, *101*, 12,667–12,683, 1996.

Rind, D., R. Suozzo, N. K. Balachandran, A. Lacis, and G. L. Russell, The GISS Global Climate/Middle Atmosphere Model, I, Model structure and climatology, *J. Atmos. Sci.*, *45*, 329–370, 1988.

Rind, D., R. Suozzo, N. K. Balachandran, and M. Prather, Climate change and the middle atmosphere, 1, The doubled CO_2 climate, *J. Atmos. Sci.*, *47*, 475–494, 1990.

Rind, D., D. Shindell, P. Lonergan, and N. K. Balachandran, Climate change and the middle atmosphere, III, The doubled CO_2 climate revisited, *J. Clim.*, *11*, 876–894, 1998.

Rind, D., J. Lerner, K. Shah, and R. Suozzo, Use of on-line tracers as a diagnostic tool in general circulation model development, 2, Transport between the troposphere and stratosphere, *J. Geophys. Res.*, *104*, 9151–9167, 1999.

Rind, D., J. Lerner, and C. McLinden, Changes of tracer distributions in the doubled CO_2 climate, *J. Geophys. Res.*, *106*, 28,061–28,079, 2001.

Rind, D., P. Lonergan, N. K. Balachandran, and D. Shindell, 2xCO_2 and solar variability influences on the troposphere through wave-mean flow interactions, *J. Meteorol. Soc. Jpn.*, *80*, 863–876, 2002.

Senior, C. A., The dependence of climate sensitivity on the horizontal resolution of a GCM, *J. Clim.*, *8*, 2860–2880, 1995.

Shindell, D., D. Rind, and P. Lonergan, Climate change and the middle atmosphere, IV:1, Ozone photochemical response to doubled CO_2, *J. Clim.*, *11*, 895–918, 1998.

Shindell, D., R. Miller, G. Schmidt, and L. Pandolfo, Simulation of recent northern winter climate trends by greenhouse-gas forcing, *Nature*, *399*, 452–455, 1999.

Tegen, I., and R. Miller, A general circulation model study on the interannual variability of soil dust aerosol, *J. Geophys. Res.*, *103*, 25,975–25,995, 1998.

Thompson, D. W., J. M. Wallace, and G. C. Hegerl, Annular modes in the extratropical circulation, II, Trends, *J. Clim.*, *13*, 1018–1036, 2000.

Yao, M.-S., and A. D. Del Genio, Effects of cloud parameterization on the simulation of climate changes in the GISS GCM, *J. Clim.*, *12*, 761–779, 1999.

Zorita, E., and F. Gonzalez-Rouco, Disagreement between predictions of the future behavior of the Arctic Oscillation as simulated in two different climate models: Implications for global warming, *Geophys. Res. Lett.*, *27*, 1755–1758, 2000.

J. Lerner, J. Perlwitz, and D. Rind, Goddard Institute for Space Studies at Columbia University, 2880 Broadway, New York, N.Y. 10025, USA. (jlerner@giss.nasa.gov;judith@giss.nasa.gov;drind@giss.nasa.gov)

C. McLinden, Air Quality Research Branch, Meteorological Service of Canada, 4905 Dufferin Street, Toronto, ON M3H 5T4, Canada. (chris.mclinden@ec.gc.ca)

M. J. Prather, Earth System Science Department, University of California, Irvine, Irvine, CA 92697-3100, USA. (mprather@uci.edu)